

Article

Hydrogenation and Hydrodeoxygenation of Oxygen-Substituted Aromatics over Rh/silica: Catechol, Resorcinol and Hydroquinone

Kathleen Kirkwood and S. David Jackson * 

Centre for Catalysis Research, School of Chemistry, University of Glasgow, Glasgow G12 8QQ, UK; k.kirkwood.1@research.gla.ac.uk

* Correspondence: david.jackson@glasgow.ac.uk; Tel.: +44-(0)141-330-4443

Received: 7 May 2020; Accepted: 18 May 2020; Published: 22 May 2020



Abstract: The hydrogenation and hydrodeoxygenation (HDO) of dihydroxybenzene isomers, catechol (1,2-dihydroxybenzene), resorcinol (1,3-dihydroxybenzene) and hydroquinone (1,4-dihydroxybenzene) was studied in the liquid phase over a Rh/silica catalyst at 303–343 K and 3 barg hydrogen pressure. The following order of reactivity, resorcinol > catechol > hydroquinone (*meta* > *ortho* > *para*) was obtained. Kinetic analysis revealed that catechol had a negative order of reaction whereas both hydroquinone and resorcinol gave positive half-order suggesting that catechol is more strongly adsorbed. Activation energies of ~ 30 kJ·mol⁻¹ were determined for catechol and hydroquinone, while resorcinol gave a value of 41 kJ·mol⁻¹. Resorcinol, and similarly hydroquinone, gave higher yields of the hydrogenolysis products (cyclohexanol, cyclohexanone and cyclohexane) with a cumulative yield of $\sim 40\%$. In contrast catechol favoured hydrogenation, specifically to cis-1,2-dihydroxycyclohexane. It is proposed that cis-isomers are formed from hydrogenation of dihydroxycyclohexenes and high selectivity to cis-1,2-dihydroxycyclohexane can be explained by the enhanced stability of 1,2-dihydroxycyclohex-1-ene relative to other cyclohexene intermediates of catechol, resorcinol or hydroquinone. Trans-isomers are not formed by isomerisation of the equivalent cis-dihydroxycyclohexane but by direct hydrogenation of 2/3/4-hydroxycyclohexanone. The higher selectivity to HDO for resorcinol and hydroquinone may relate to the reactive surface cyclohexenes that have a C=C double bond β - γ to a hydroxyl group aiding hydrogenolysis. Using deuterium instead of hydrogen revealed that each isomer had a unique kinetic isotope effect and that HDO to cyclohexane was dramatically affected. The delay in the production of cyclohexane suggest that deuterium acted as an inhibitor and may have blocked the specific HDO site that results in cyclohexane formation. Carbon deposition was detected by temperature programmed oxidation (TPO) and revealed three surface species.

Keywords: catechol; resorcinol; hydroquinone; Rh/silica; hydrogenation; hydrodeoxygenation; deuterium

1. Introduction

Lignocellulosic biomass can be converted into liquid bio-oil via fast pyrolysis at 673–873 K in the absence of air with multiple reactions taking place, which results in a bio-oil that contains over 300 individual compounds. However, the presence of multiple oxygenates and resultant low heating value, corrosiveness, high viscosity and instability limits commercial viability [1–4]. Up until now, efforts to remove this oxygen selectively have focused on high temperature (>473 K) catalytic hydrodeoxygenation (HDO), with Ni or Co supported catalysts most commonly employed [5,6]. Although active for HDO, significant deactivation occurs with these catalysts resulting in a shift in research towards noble metals. In this paper, we will report on the hydrogenation and low

temperature (<373 K) hydrodeoxygenation of catechol, resorcinol and hydroquinone. In general, the dihydroxybenzenes have received considerably less attention than phenol, guaiacol and anisole as model compounds representing bio-oil, of the three, catechol hydrodeoxygenation has received the most attention. Studies by Song et al. [7] at 473 K over a Ni catalyst recorded 12% yield of phenol after 2 h with the ring hydrogenated product cyclohexane-1,2-diol being the major product (85% yield). Through the course of their study, benzene, the complete HDO product, was undetected [7]. They proposed a mechanism whereby aryl C–O bond hydrogenolysis and aromatic ring hydrogenation occurred in parallel, where the latter reaction dominated. However, Zhao et al. [8] suggested catechol underwent direct hydrogenolysis to phenol with subsequent hydrogenation to cyclohexanone and cyclohexanol. They observed cyclohexane-1,2-diol undergo hydrogenolysis to cyclohexanone and cyclohexanol at 523 K suggesting a higher temperature barrier required to cleave the aliphatic–OH than the aromatic–OH [8]. A study examining all three dihydroxybenzene isomers over a 5% rhodium/alumina catalyst found the order of reactivity: hydroquinone > resorcinol > catechol, where catechol underwent the least cleavage proposed as a consequence of steric inhibition in the *ortho* position [9].

Studies of dihydroxybenzenes on the effect of symmetry, number of substituents, relative rates and reaction order have recorded similar but by no means uniform trends to that observed with xylenes. It is generally thought that for compounds with the same number of substituents those with symmetrical arrangement have the highest rate, with the order of reactivity of the dihydroxybenzenes believed to follow a similar pattern to the xylene isomers: *para* > *meta* > > *ortho*-xylene found by Vannice and Rahman [10,11]. A study by Jackson et al. [12], however, reported an order of xylenes that followed *para* > *ortho* > *meta*, with Furimsky et al. [13] reporting an order in reactivity: *meta* > *para* > *ortho* for substituted phenols. It is clear from current literature that no clear correlation exists between number and symmetry of substituents on reaction rate.

The bulk of the literature up until now has reported HDO as occurring at high temperature and pressure, however, a recent study examining phenol hydrogenation over rhodium at low temperature and pressure (≤ 343 K, 2–5 barg hydrogen) found a 20% yield of cyclohexane [14]. In light of this, the occurrence of dihydroxybenzene hydrogenolysis under similar conditions was a possibility and worthy of investigation.

2. Results and Discussion

2.1. Hydrogen Reactions

Extra reaction profiles and data analysis are contained in the Supplementary Data File. To ascertain activation energies and order in reactants, hydrogenation was carried out over a range of temperatures and concentrations (Table 1). From Table 1 it can be seen the order of reactivity followed: resorcinol > catechol > hydroquinone and the strength of adsorption based on the order of reaction in organic followed: catechol > hydroquinone > resorcinol. Xylene hydrogenation over a similar catalyst gave an order of reactivity of *para* > *ortho* > *meta*, which is the reverse of that found with dihydroxybenzenes [12], while the hydrogenation of dimethoxybenzenes over a rhodium catalyst gave an order of activity of *para* > *meta* > *ortho* [15], indicating that changing the substituents results in a change in the ordering of the reactivity of the isomers. It has been reported that replacing a methyl substituent with a hydroxyl substituent reduces the reactivity of an aromatic species [16] and, indeed, we have found that dihydroxybenzenes are less reactive than the equivalent xylene [12], which may be due to the strength of adsorption. With alkylbenzenes, as the inductive effect increases so does the strength of adsorption resulting in a decrease in the rate of hydrogenation [12]; therefore, as electron donation to the aromatic ring is greater for hydroxyl groups than methyl groups, adsorption of dihydroxybenzenes should be stronger and the rate of hydrogenation slower.

Table 1. Kinetic data for hydrogenation of catechol, resorcinol and hydroquinone.

Compound	E _a (kJ·mol ⁻¹)	Order in Organic	k ^a (min ⁻¹ , ×10 ⁻³)
Catechol	29 ± 1	-0.29 ± 0.01	8.3
Resorcinol	41 ± 4	0.60 ± 0.09	11.2
Hydroquinone	31 ± 5	0.41 ± 0.06	4.2

^a k, first order rate constant measured at 323 K, 3 barg and ~10 mmol reactant.

The activation energies for all three substrates were in the range 29–41 kJ mol⁻¹, in agreement with a previous study over a Rh catalyst [9]. It was found that resorcinol had the fastest rate of reaction, with the major products (cyclohexanol and cyclohexanone) formed through direct HDO of resorcinol (Figure 1).

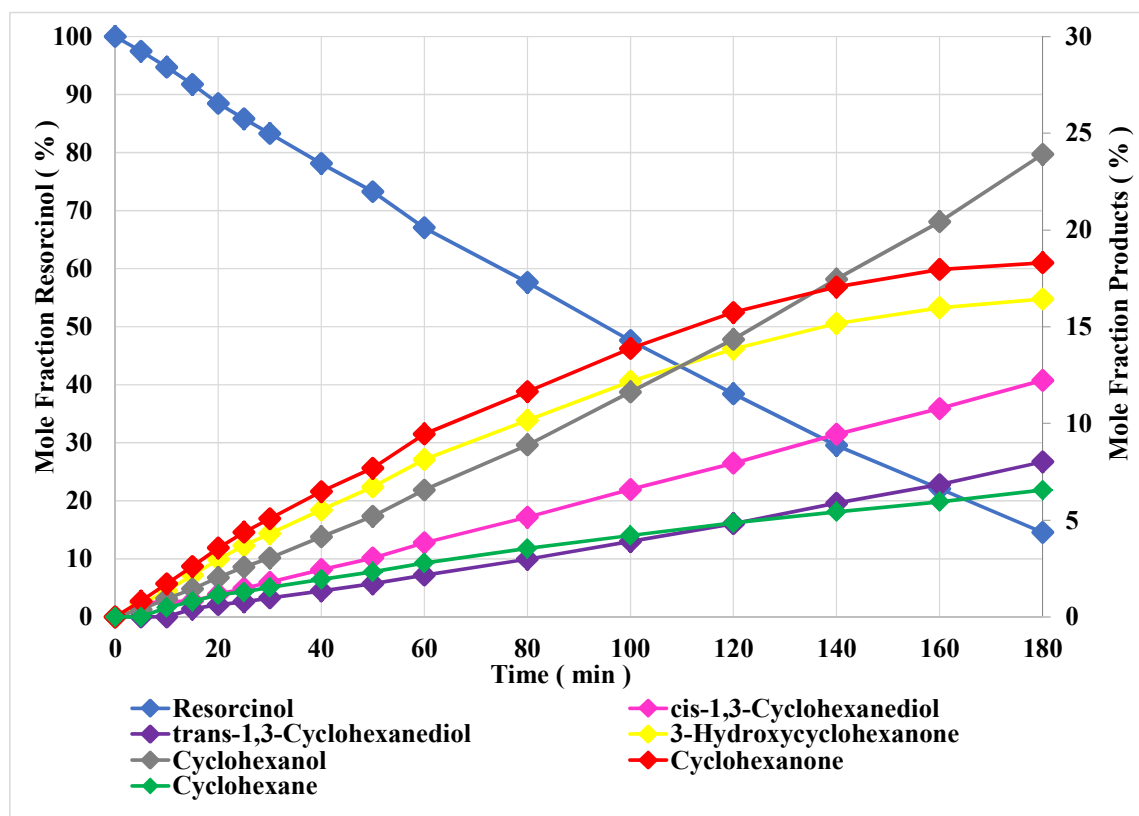


Figure 1. Reaction profile of resorcinol hydrogenation. Conditions, 323 K, 10 mmol, 3 barg.

The major product of the reaction was the hydrogenolysis/HDO product, cyclohexanol, at ~24%, with the ring hydrogenated products, isomers of cyclohexanediol and hydroxycyclohexanone, formed to a lesser extent (12% *cis* and 8% *trans* and 16%, respectively). It was not expected that preferential formation of the HDO product, cyclohexanol, would occur under such mild conditions as the majority of HDO studies operate at elevated temperature and pressure (>473 K and >10 barg hydrogen) in the belief that cleavage of the Ar-OH bond in bio-oil requires harsh conditions. The hydrogenation of resorcinol did not reach completion at 323 K within 180 min, however at 333 K and 343 K reaction did reach completion by 140 and 160 min, respectively (Supplementary Material, Figure S2 and Figure 2). From Figure 2, it is apparent that both cyclohexanone and 3-hydroxycyclohexanone were formed as intermediates, hydrogenating further to cyclohexanol and cyclohexanediol isomers, respectively. It can be seen that the two cyclohexanone intermediates initially had the highest selectivities, being formed directly from resorcinol. Their levels increased steadily over 80 min before decreasing as they were hydrogenated and not replaced from resorcinol.

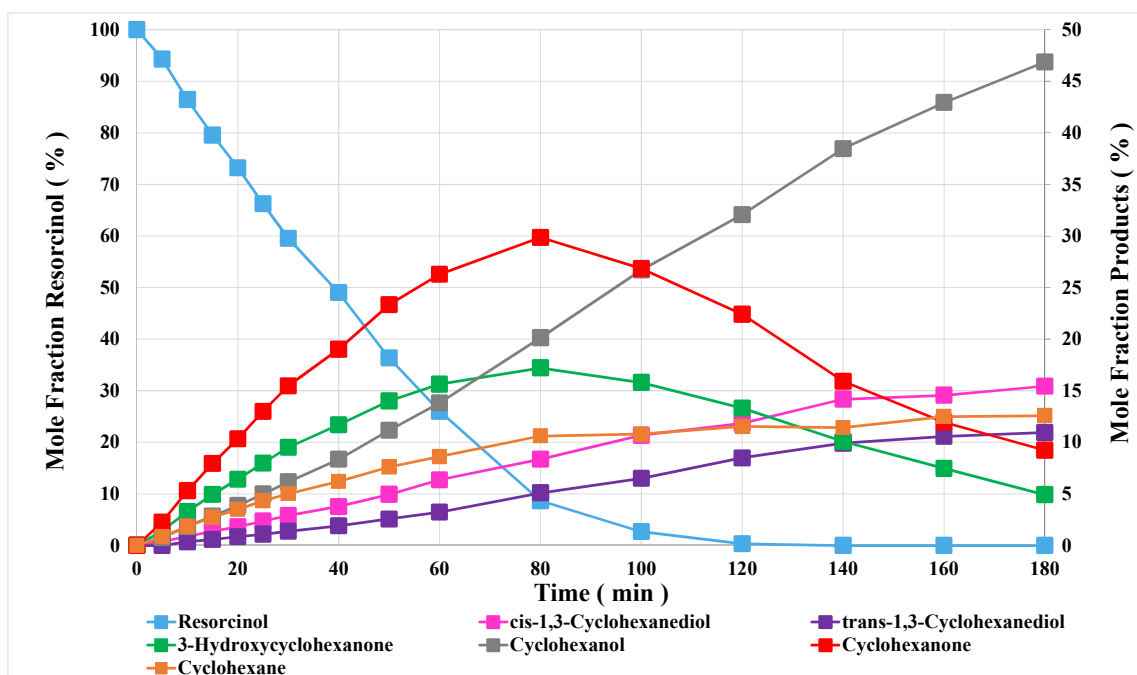


Figure 2. Reaction profile of resorcinol hydrogenation. Conditions, 343 K, 10 mmol, 3 barg.

The hydrogenation/HDO routes are shown in Figure 3. It has been suggested that cyclohexane is formed from cyclohexanol [17], however other authors [18] have suggested direct conversion of phenol to cyclohexane. We have shown that cyclohexanol is stable under these conditions [14] and does not form cyclohexane, therefore cyclohexane is a direct product from resorcinol. As may be expected, an increase in temperature resulted in higher selectivity to hydrogenolysis products as shown in Figure 4. Similar behaviour was reported with anisole hydrogenation over rhodium [14].

The *para* isomer, hydroquinone, although exhibiting similar behaviour to resorcinol showed a significantly reduced rate of reaction as can be seen in Figure 5. This lower rate of reaction for the *para* isomer is rarely documented; instead it is generally reported to have the highest reactivity due to its symmetrical arrangement. A study of xylene isomers found *para*-xylene to have the highest reactivity [12], however the presence of two strongly electron donating groups on the dihydroxybenzenes may influence this order. The product distribution for hydroquinone was closely related to that of resorcinol with cyclohexanol the major product at 180 min. At 70% conversion of both resorcinol and hydroquinone, the cumulative yield of hydrogenolysis products was ~40% compared to ~30% for hydrogenated only products. The formation of the hydrogenolysis product cyclohexane (~8% yield) was particularly significant at these conditions, as it required the aromatic to undergo hydrogenation and two bond cleavages to remove both -OH groups. By comparison the hydrogenation of phenol over a similar catalyst gave ~16% yield of cyclohexane at 70% conversion, showing that the process is slower with two hydroxyl substituents in a *para* configuration [14].

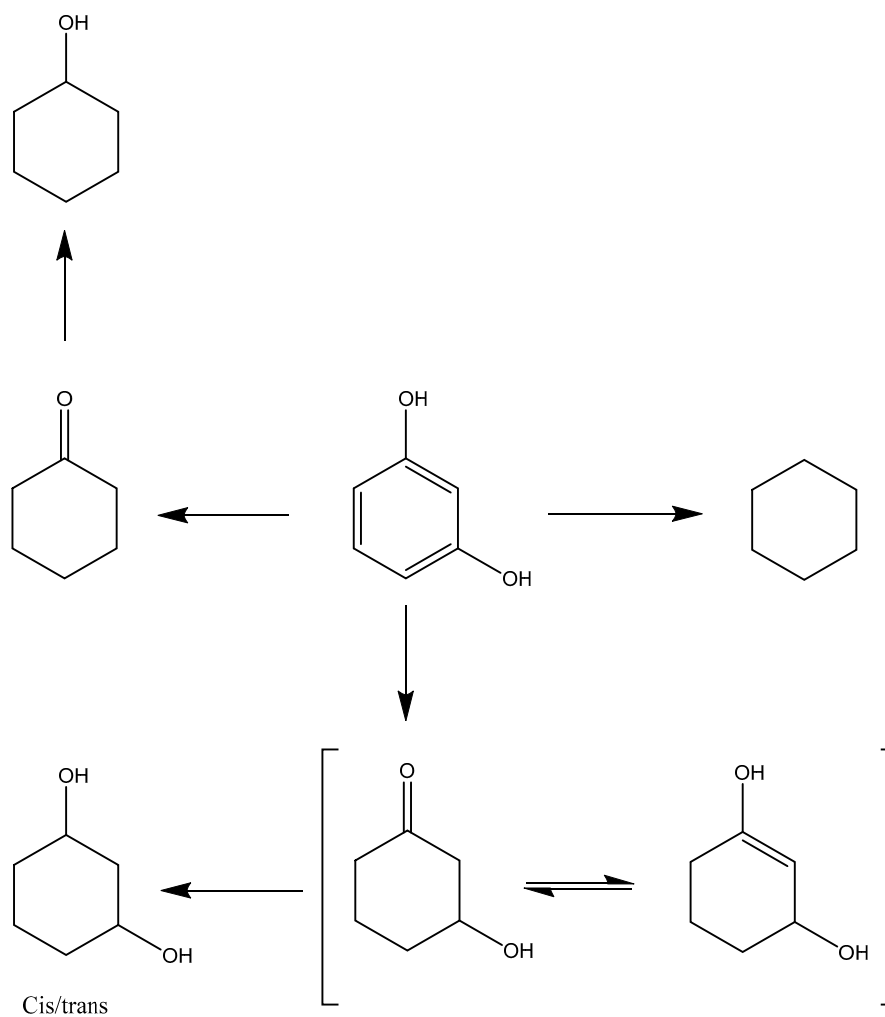


Figure 3. Hydrogenation and HDO routes from resorcinol.

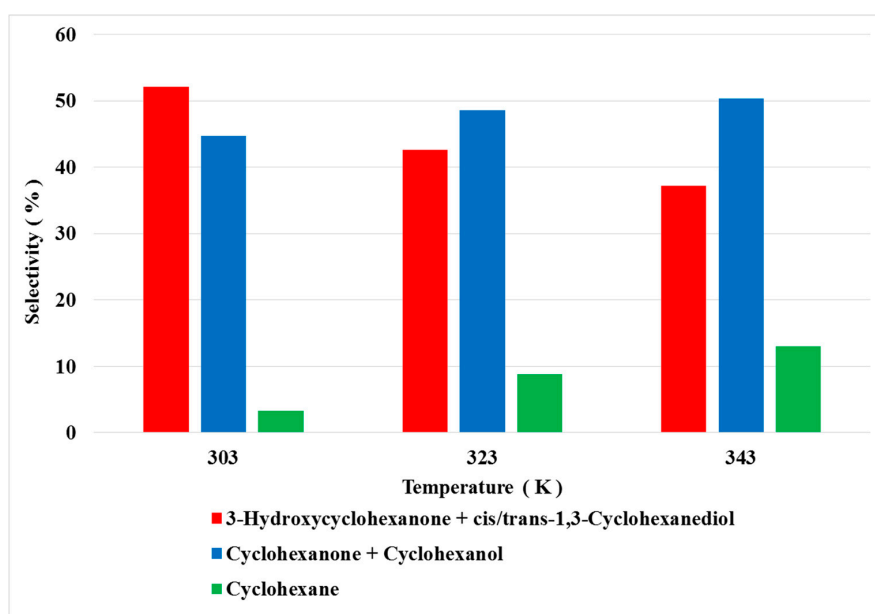


Figure 4. Selectivity obtained from resorcinol hydrogenation as a function of temperature. For comparison resorcinol conversion was ~35% at each reaction temperature. Pressure 3 barg, 10 mmol.

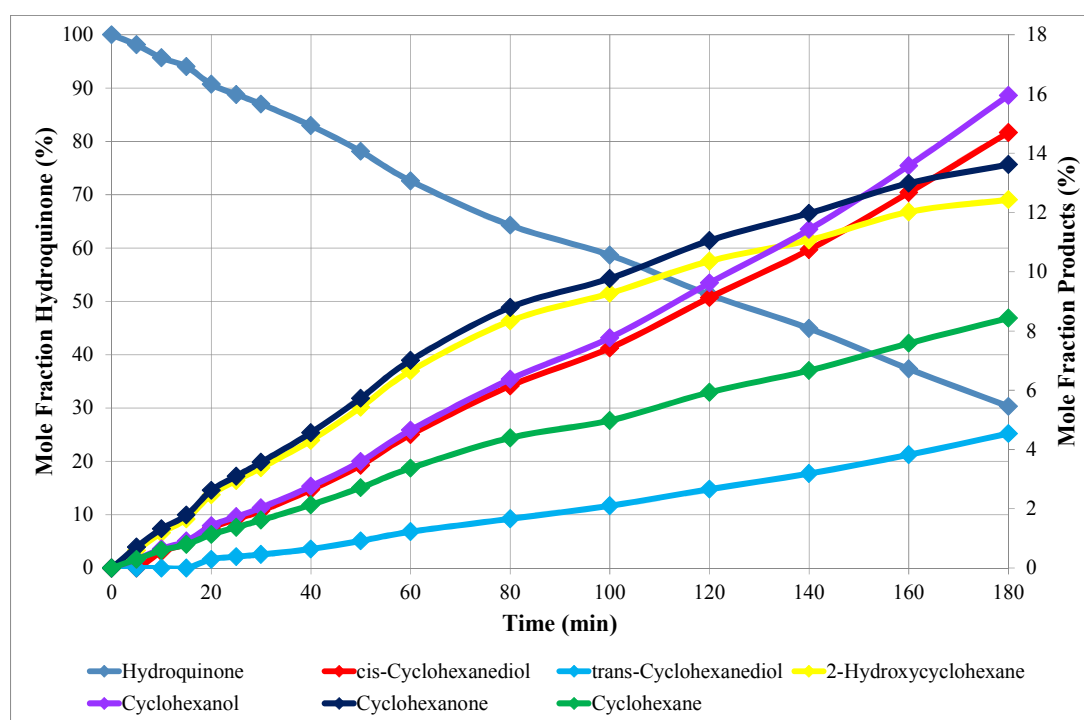


Figure 5. Reaction profile of hydroquinone hydrogenation. Conditions, 323 K, 10 mmol, 3 barg.

From Figure 6 it is clear that the *ortho*-isomer, catechol, shows significantly different behaviour from the other two isomers. In contrast to *meta* and *para*-isomers, the major products from catechol hydrogenation were the ring hydrogenated *cis*-1,2-cyclohexanediol and 2-hydroxycyclohexanone, with selectivity to the *cis*-isomer of ~33% compared to ~13% from resorcinol and hydroquinone. As mentioned previously, Song et al. [7] studied catechol HDO over a Ni catalyst at elevated conditions, and recorded the major product as cyclohexanediol, in agreement with our findings. However, Song et al. detected the presence of phenol (~12% yield) which was not observed in our study. Similarly, they saw no formation of benzene, postulated to be the result of a lower C-O hydrogenolysis barrier for catechol compared to phenol. The rate of phenol hydrogenation [14] was significantly faster than that of the dihydroxybenzenes in our study ($k_{\text{phenol}} 14.7 \times 10^{-3} \text{ min}^{-1}$ c.f. $k_{\text{resorcinol}} 11.2 \times 10^{-3} \text{ min}^{-1}$). It is however, well documented that an increase in the number of substituents on the aromatic ring decreases the rate of reaction [19,20].

From Figure 6 it can be seen that the formation of HDO products from catechol occurred to a lesser extent than observed with hydroquinone and resorcinol, for example, at ~80% conversion of catechol, cyclohexanol yield was ~8% compared to ~19% for resorcinol hydrogenation at a similar conversion. This significant decrease in -OH group cleavage on moving one position on the aromatic ring may be an effect of the close proximity of the two substituents, which can facilitate interaction between the two-hydroxyl groups via hydrogen bonding, resulting in further suppression of the deoxygenation capability of the *ortho*- isomer. Figure 7 clearly demonstrates these differences in levels of hydrogenation and hydrogenolysis product formation between the three isomers with resorcinol and hydroquinone showing a preference to HDO whilst catechol favours hydrogenation. This markedly different behaviour of the *meta* and *para*-isomers relative to the *ortho*-isomer may be due to an adsorption effect. Literature on dihydroxybenzenes adsorption interactions is sparse. Studies by Odebunmi and Ollis on HDO of substituted phenols found similar behaviour with methyl substituted phenols, where the *ortho*-methyl phenol exhibited a greater resistance to HDO than the *meta/para*-methyl phenols [21,22]. Hence, it is possible that the main factor determining the deoxygenation ability of *para/meta*-isomers as against *ortho*-isomer is the mode of adsorption of the substrate. The assumption made by many is that *para*- and *meta*-isomers both have a flat mode of adsorption whereas the *ortho*

isomer adopts an inclined mode as postulated by Bredenberg and Sarbak [23] in a study of the adsorption of dihydroxybenzenes using chemisorption and infrared spectroscopy. However, a flat mode of adsorption for dihydroxybenzenes is possible in the *ortho* position, bonded strongly through the two oxygen atoms, with the hydrogen atoms pointing away from the surface to give a mode of adsorption similar to that of the *meta*- and *para*-isomers. Rather than mode of adsorption, it may be the proximity and strength of bonding in the *ortho* position that significantly suppresses the cleavage of the –OH. However, the substitution of an –OH for a –CH₃ group would result in the inclined mode of adsorption discussed. A study by Furimsky et al. [13] examined the effect of the addition of a methyl substituent and found a decrease in rate and an increase in the resistance of the ring to undergo hydrogenation. They attributed these findings to a possible steric effect in the transient state between the reactant and catalyst surface.

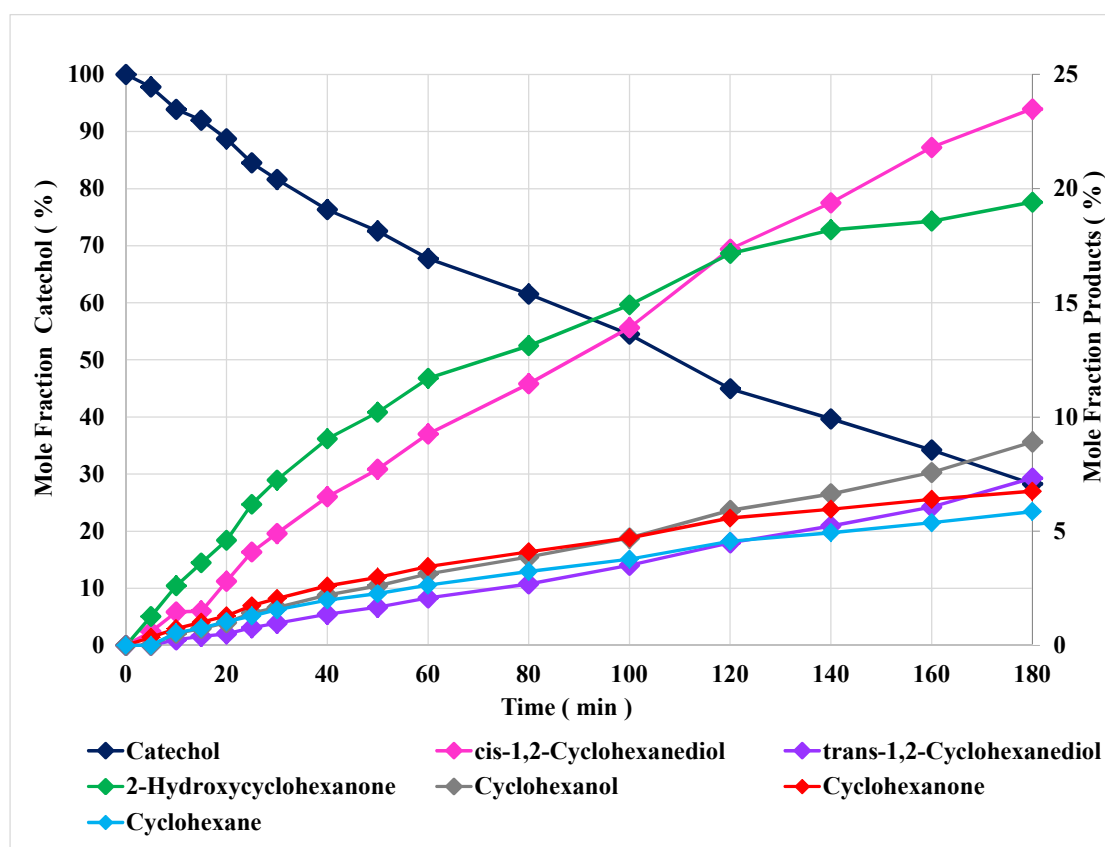


Figure 6. Reaction profile of catechol hydrogenation. Conditions, 323 K, 10 mmol, 3 barg.

The rate of hydrogenation for the dihydroxybenzenes gave an order of resorcinol > catechol > hydroquinone (*meta* > *ortho* > *para*), in contrast to that reported in literature by Smith and Stump over rhodium and platinum catalysts in a sealed reactor, where the order was given as (*para* > *meta* > *ortho*) [9]. However, their results do agree that catechol undergoes less hydrogenolysis than hydroquinone or resorcinol. Nevertheless, the higher activity for resorcinol in comparison to the other two isomers found in our study has been documented previously in a study by Maximov et al. [24] over a ruthenium catalyst, where the favourable arrangement of the two hydroxy groups in the *meta* position was postulated as the reason behind the faster rate. Furthermore, a study of HDO of methyl substituted phenols by Furimsky. et al. [13] also found the *meta*-isomer to be the most reactive isomer followed in that instance by the *para*-isomer.

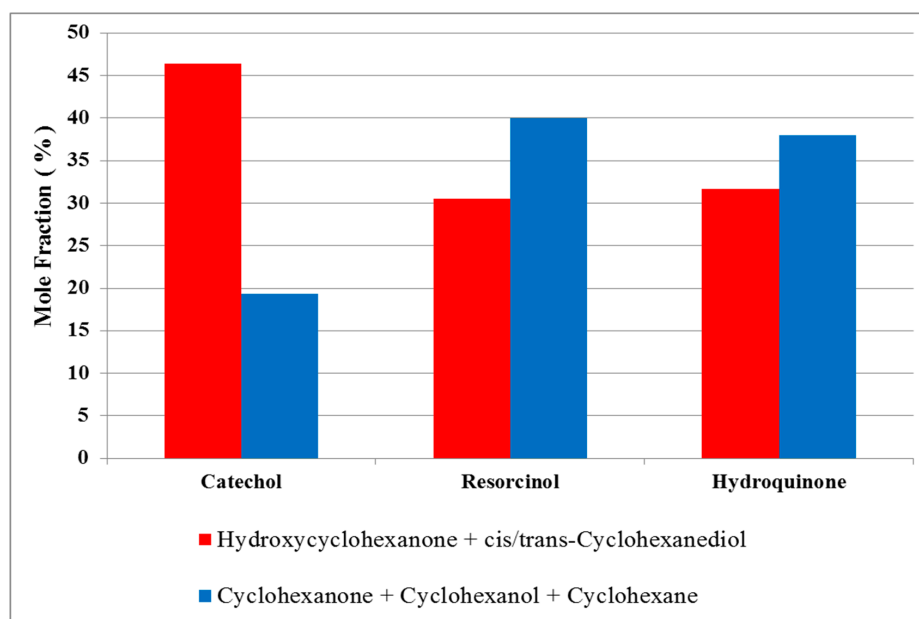


Figure 7. Comparison of hydrogenation and HDO at 323 K of catechol, resorcinol and hydroquinone at ~70% conversion (Hydroxycyclohexanone + *cis/trans*-cyclohexanediol are summed to be representative of hydrogenation, while cyclohexanone, cyclohexanol + cyclohexane are summed to be representative of HDO). Pressure 3 barg, 10mmol.

A study of phenol hydrogenation under similar reaction conditions recorded a yield of the HDO product, cyclohexane of ~20%, double that found in our study [20]. The formation of cyclohexane from phenol, however, requires the cleavage of only one –OH group, whereas for dihydroxybenzene cleavage of two –OH groups is necessary. The different bond dissociation energies of aromatic and aliphatic C–O bonds, 468 and 385 kJ·mol⁻¹, respectively, with the greater energy required to cleave the aromatic-OH bond, used to suggest that initial hydrogenation followed by subsequent hydrogenolysis is the route of –OH bond cleavage [13]. However, hydrogenation of cyclohexanone found cyclohexanol as the sole product, with no cyclohexane detected [14] and cyclohexanol was stable under reaction conditions. Both these findings suggest a direct route of cyclohexane formation from the aromatic [14]. To confirm that HDO was not via a hydrogenated species, *cis*-1,2-cyclohexanediol was used as the reactant and subjected to standard reaction conditions for 3 h: no cyclohexane or cyclohexanol was detected (The reaction graph can be found in Figure S9 of the Supplementary Information Section). Therefore, we propose that the formation of the hydrogenolysis products occurs directly from the aromatic via highly reactive surface intermediates. This idea of reactive surface intermediates being linked to HDO activity was first stated by Smith and Stump during their study on dihydroxybenzene hydrogenation [9]. The initial hydrogenation of the aromatic results in the formation of highly reactive surface intermediates, containing double bonds, which facilitate the promotion of hydrogenolysis. Examining catechol as an example and considering the intermediates that can be formed (Figure 8) it is apparent that intermediates A and D contain a double-bond β-γ to a hydroxyl group, rendering this group susceptible to hydrogenolysis. Intermediate B is the most stable configuration for the double bond and is likely the major route for the formation of 2-hydroxycyclohexanone through *keto-enol* tautomerism. Intermediate D also has the potential to form 2-hydroxycyclohexanone through *keto-enol* tautomerism. Further hydrogenation of 2-hydroxycyclohexanone would result in the formation of *cis/trans*-1,2-cyclohexanediol and as such, intermediates B and D are the most likely routes for hydrogenation. It should be noted that although intermediate A can form the HDO products via hydrogenolysis, it can also form the hydrogenated products. Intermediate C is unlikely to contribute significantly to the reaction due to the position of its double bond. When studying intermediate formation for resorcinol and hydroquinone it is apparent that a greater number of those with a

double-bond β - γ to the hydroxyl group, as seen above in A, can be potentially formed, which may explain the increased bias towards hydrogenolysis observed with these two isomers.

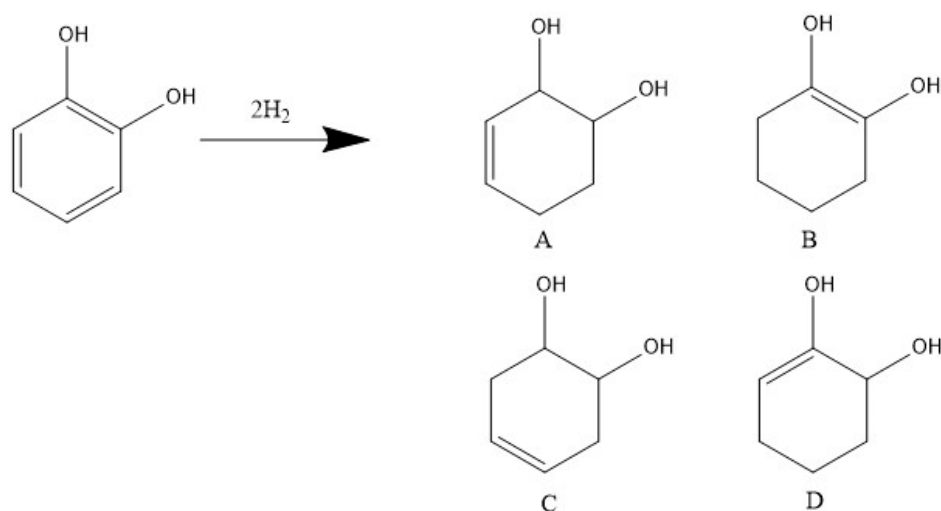


Figure 8. Catechol hydrogenation via highly reactive intermediates.

Further differences in behaviour of the three dihydroxybenzenes substrates was apparent in the *cis:trans* ratio of the cyclohexanediol product. As expected all three preferentially formed the *cis* isomer, however, the *cis:trans* ratios of the cyclohexanediols formed from catechol and hydroquinone were significantly greater than that observed with resorcinol as can be seen in Figure 9. This is slightly surprising as the ring position of substituents dictates that it is thermodynamically more favourable for the *trans*-isomer to form with catechol and hydroquinone, whereas our results show that *trans*-isomer is being formed more favourably with resorcinol.

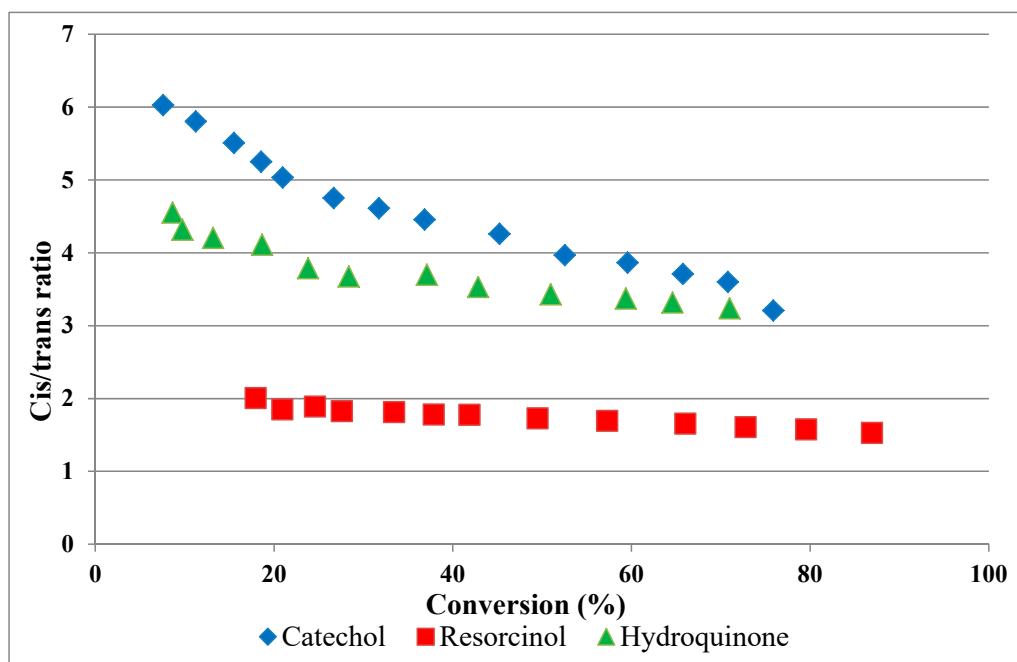


Figure 9. *Cis/trans* ratio as a function of conversion for the three isomers.

This raises the question of how the *trans*-isomer is formed. No isomerisation or hydrogenolysis was observed when *cis*-1,2-dihydroxycyclohexane was used as reactant indicating that the *trans*-isomer is not formed by subsequent isomerisation of the *cis*-isomer, thereby necessitating a direct route

to the *trans*-isomer. The *cis*-isomer can be formed through hydrogenation of the enol form of hydroxycyclohexanone (i.e., 1,2-dihydroxycyclohex-1-ene, intermediate B in Figure 8). Note that this would explain the high yield of *cis*-1,2-cyclohexanol compared to the 1,3- and 1,4-isomers as only catechol can produce a four-substituted alkene as an intermediate, which will be more stable and hence have a greater chance of hydrogenation relative to tautomerism to the keto-form. In contrast we propose that the *trans*-isomer is formed solely via hydrogenation of hydroxycyclohexanone via desorption and subsequent re-adsorption. Hydrogenation of the C=O functionality will be slower than hydrogenation of the C=C functionality hence the *trans*-isomer is always formed later in the reaction than the *cis*-isomer.

2.2. Deuterium Reactions

To further explore the mechanism of hydrogenation and hydrodeoxygenation, in the following set of reactions, deuterium was used in place of hydrogen for both the reduction and reaction procedure. All other parameters were set as per standard conditions (323 K, 10 mmol substrate, and 3 barg pressure). Comparison of the rate constants from reactions carried out in deuterium and hydrogen was used to calculate the kinetic isotope effect for each substrate. The reaction profiles are shown in Figures 10–12. The results suggested significant mechanistic differences between the reactions of the dihydroxybenzenes. Table 2 show the kinetic isotope effects.

Table 2. Kinetic isotope effect (KIE) for the individual dihydroxybenzene isomer reactions.

Substrate	k_H^a ($\text{min}^{-1}, \times 10^{-3}$)	k_D ($\text{min}^{-1}, \times 10^{-3}$)	$\text{KIE} = \frac{k_H}{k_D}$
Resorcinol	11.9	12.5	0.9
Hydroquinone	4.2	2.9	1.5
Catechol	8.3	12.8	0.6

^a k , first order rate constant measured at 323 K, 3 barg and ~10 mmol reactant.

Comparing Figure 1 with Figure 10 it is clear that resorcinol showed a faster rate of reaction under deuterium with the conversion after 180 min increasing from 86% under hydrogen to ~96% under deuterium. A marked difference in the production of cyclohexane was observed with a delay of 30 min when using deuterium whereas when using hydrogen, cyclohexane formation occurred immediately.

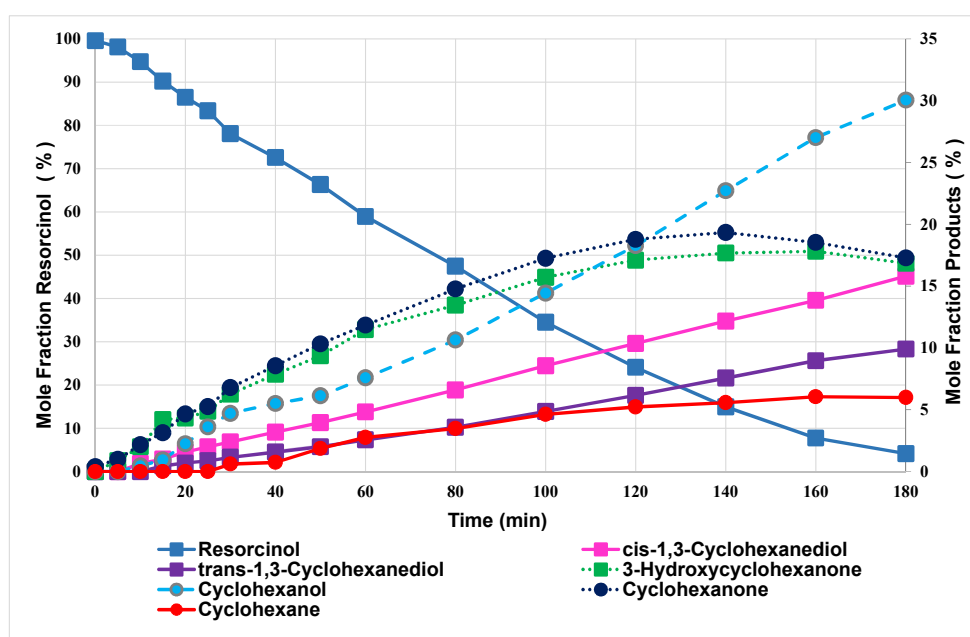


Figure 10. Deuteration of resorcinol. Conditions: 323 K, 3 barg D_2 , 10 mmol resorcinol.

Comparing Figure 5 with Figure 11 it is clear that in, contrast to resorcinol, hydroquinone had a slower rate of reaction under deuterium with the conversion after 180 min decreasing from 70% under hydrogen to ~76% under deuterium. A similar inhibition in the production of cyclohexane was observed with a delay of 20 min when using deuterium whereas when using hydrogen, cyclohexane formation occurred immediately.

The reaction of catechol under deuterium (Figure 12) had a significantly higher rate than under hydrogen, resulting in a marked inverse kinetic isotope effect. A similar inhibition to that found with the other dihydroxybenzenes isomers regarding the production of cyclohexane was observed with a delay of 20 min when using deuterium.

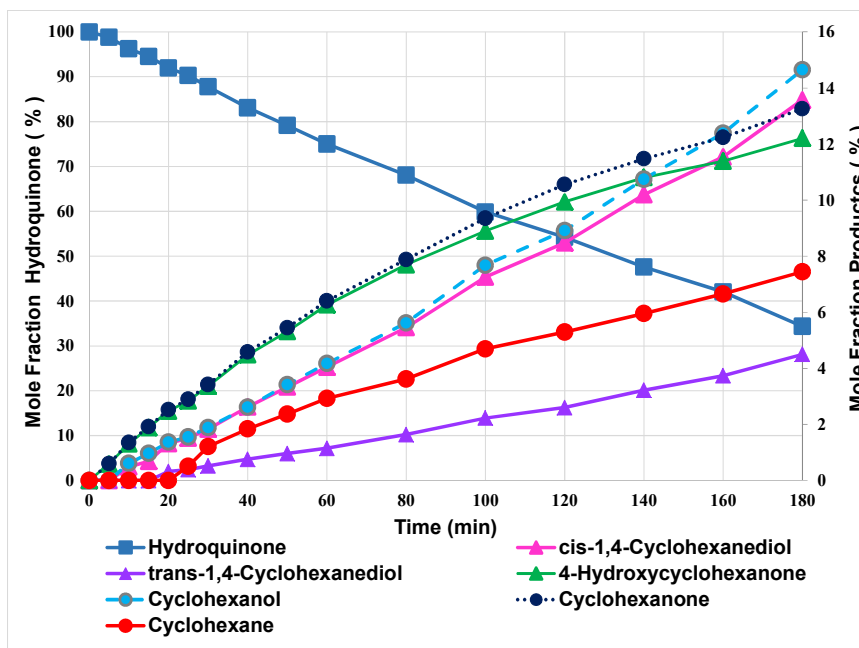


Figure 11. Deuteration of hydroquinone. Conditions: 323 K, 3 barg D₂, 10 mmol

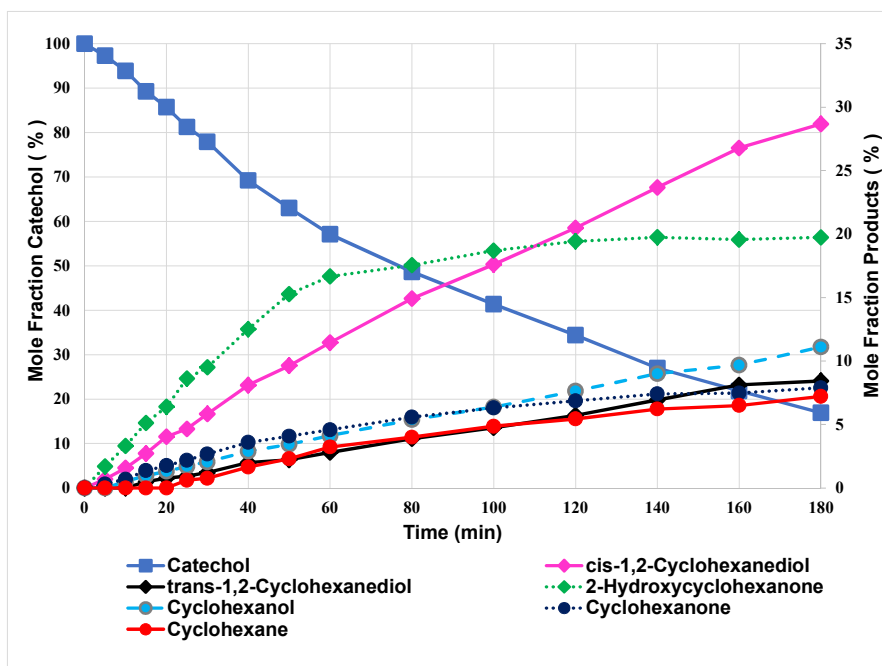


Figure 12. Deuteration of catechol. Conditions: 323 K, 3 barg D₂, 10 mmol catechol.

We could find no literature directly related to the use of deuterium to hydrogenate dihydroxybenzenes; however, hydrogen-deuterium studies of phenol, anisole and 4-methoxyphenol have been reported [14]. Both phenol and anisole gave standard kinetic isotope effects but 4-methoxyphenol gave an inverse kinetic isotope effect (KIE), which is in contrast to hydroquinone (4-hydroxyphenol) in this study which gave the only positive KIE. Clearly the change from $-OH$ to $-OCH_3$ resulted in a change of mechanism. The deuteration of alkyl-substituted benzenes has been reported [12]. A comparison of hydrogenation and deuteration of toluene, ethylbenzene and propyl benzene revealed that all three displayed an inverse kinetic isotope effect, which was concluded to be due to the change in hybridisation of the carbon atom from sp^2 to sp^3 which takes place during the hydrogenation of the aromatic ring—an explanation which may explain the inverse KIE values calculated for catechol and resorcinol. A study on xylenes hydrogenation [12] also found a disparity amongst isomers, however in this instance the *ortho*-isomer exhibited a positive KIE and while the *meta*- and *para*-isomers displayed an inverse KIE. It was concluded the *ortho*-xylene must have a different rate-determining step (RDS) from the *meta*- and *para*-xylene. In our study, something similar may apply with both catechol and resorcinol having a different RDS from hydroquinone. This was a surprise as resorcinol and hydroquinone exhibited similar hydrogenation/HDO behaviour.

One common feature to all three isomers is the delay in cyclohexane formation. Under our reaction conditions no benzene or phenol is detected and cyclohexanol is stable, therefore cyclohexane is formed directly from dihydroxybenzene. As cyclohexane is formed directly it is likely that the inhibition is due to changes on the rhodium surface. It has been proposed for anisole HDO [25] that the hydrodeoxygenation reaction is favoured by small rhodium crystallites with reaction on the low coordination number sites. At the outset of the reaction the rhodium surface will be covered in deuterium, however as the reaction progresses the surface will contain a mixture of H and D due to exchange processes. The Rh-D bond is stronger than the Rh-H bond [26] and in deuterium exchange reactions over rhodium a delay in reaction initiating has also been observed before the reaction moved to a steady state [27] Therefore we propose that the adsorbed deuterium on the low coordination number sites inhibits the reaction until there is sufficient exchange of D for H.

2.3. Catalysts Deactivation

To investigate catalysts post-reaction, temperature programmed oxidation (TPO) of the catalysts using a TGA-MS was performed. The TGA traces are shown in the Supplementary Data, Figures S10–S12. The catalyst used for catechol hydrogenation exhibited an overall weight loss of ~6% with ~4% of this attributed to two high temperature weight losses confirmed as $m/z = 44$ (CO_2) as shown in Figure 13. Initial weight loss events between 353 and 473 K are associated with desorption of water and catechol.

The catalyst used for resorcinol hydrogenation exhibited an overall weight loss of ~6% (Figure S11) with ~3% of this attributed to two high temperature weight losses confirmed as $m/z = 44$ (CO_2) shown in Figure 14. Initial weight loss events between 353 and 473 K are associated with desorption of water and resorcinol.

The catalyst used for hydroquinone hydrogenation exhibited an overall weight loss of ~6% (Figure S12) with ~3.5% of this attributed to two high temperature weight losses confirmed as $m/z = 44$ (CO_2) shown in Figure 15. Initial weight loss events between 353 and 473 K are associated with desorption of water and hydroquinone.

All three catalysts display two evolutions of carbon dioxide at ~500 K and ~700 K. The catalysts used with resorcinol and hydroquinone also show a carbon dioxide evolution at ~475 K. A similar feature may be present in the TPO from the catalyst used with catechol but it is less well defined. These results clearly show that even at such low reaction temperatures there is detectable carbon deposition on the catalyst surface. However, the amount as a function of the reactant is small. For the catalyst used for catechol hydrogenation, the amount of carbon removed was 4%, which represents 3.33×10^{-4} moles of carbon or ~0.5% of the carbon in the feed.

The three carbon dioxide evolutions indicate three types of surface carbon, which may differ in nature and/or position on the catalyst. As the total amount of carbon deposited is greater than the amount of rhodium present on the catalyst, it is likely that at least one of the deposited species is on the support. The other two species may be associated with different sites on the rhodium surface. Note that the deposition does reduce activity; when a catalyst was re-used, without removal from the reactor, a loss in activity of ~40% was observed.

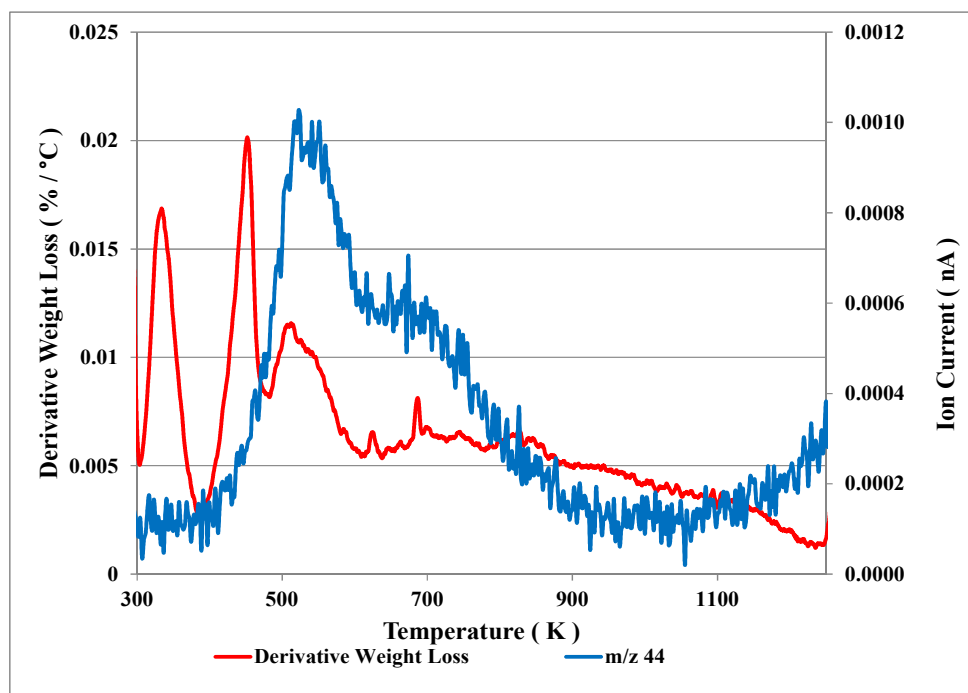


Figure 13. Derivative weight loss plotted against CO₂ evolution (m/z 44) for Rh/SiO₂ catalyst catechol hydrogenation. Conditions for reaction, 323 K, 3 barg and 10 mmol catechol.

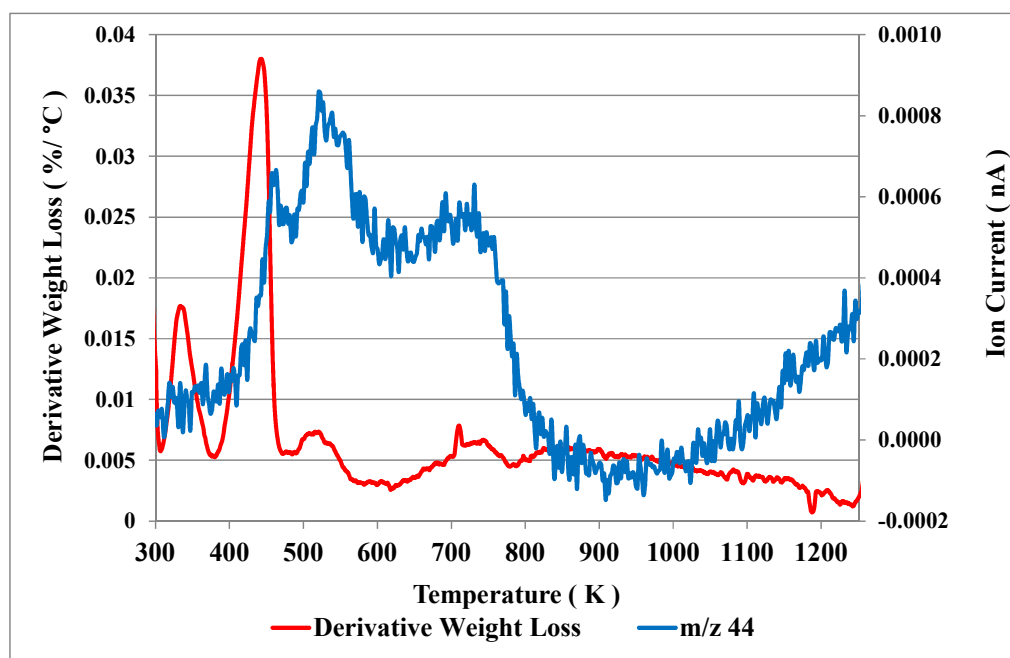


Figure 14. Derivative weight loss plotted against CO₂ evolution (m/z 44) for Rh/SiO₂ catalyst resorcinol hydrogenation. Conditions for reaction, 323 K, 3 barg and 10 mmol resorcinol.

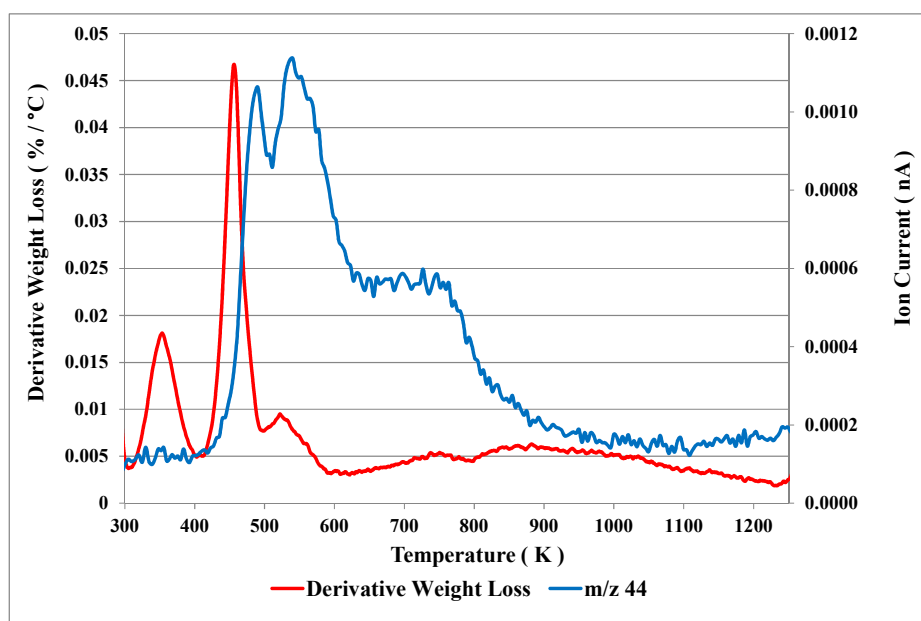


Figure 15. Derivative weight loss plotted against CO₂ evolution (*m/z* 44) for Rh/SiO₂ catalyst hydroquinone hydrogenation. Conditions for reaction, 323 K, 3 barg and 10 mmol hydroquinone.

3. Experimental

The catalyst used throughout this study (2.5% Rh/silica, M01078) was supplied and characterised by Johnson Matthey. The catalyst was prepared by employing an incipient-wetness technique using an aqueous rhodium chloride salt and a silica support supplied by Davison Catalysts. The catalysts were dried overnight at 333 K and reduced in flowing hydrogen at 473 K for 2 hours before being cooled and exposed to air. The surface area of the catalyst was 321 m²·g⁻¹ with a pore size of 13.2 nm, measured using standard BET methodology. The metal surface area was measured by hydrogen chemisorption (reproducibility ±0.5 m²·g⁻¹) and gave an area of 5.5 m²·g⁻¹ and a dispersion of 43%, from which an average metal crystallite size of 2.6 nm was calculated.

The hydrogenation reactions were performed in a 500 cm³ Büchi autoclave fitted with an oil heating jacket. The temperature was measured in the liquid slurry with accuracy of ±0.1 K and controlled by a high temperature oil circulator to ±0.5 K. The reactor was equipped with a variable speed stirrer connected to a magnetic drive that could be controlled to ±5 rpm. The pressure and gas flow was controlled by a Büchi press-flow gas controller with an accuracy of ±0.01 barg and measurement of the consumed hydrogen to 0.1 mmol. The experimental procedure involved the addition of the catalyst (100 mg Rh/SiO₂) and 310 cm³ of 2-propanol (isopropyl alcohol, IPA) into the reactor. The solvent was degassed and the autoclave purged with argon before heating to the reduction temperature. The catalyst was then reduced in situ at 343 K by sparging hydrogen gas (280 cm³ min⁻¹) through the mixture for 0.5 h, whilst stirring at 300 rpm. Once reduction was complete, the hydrogen gas and stirrer were turned off and the reactor purged with argon twice and pressurized to 1 barg. The gas controller measured the flow of hydrogen and inert gas to the reactor. Once at the desired temperature (303–343 K) the agitator was turned to 0 rpm and 10 mmol catechol (1,2-dihydroxybenzene, Sigma-Aldrich ≥99%), resorcinol (1,3-dihydroxybenzene, Sigma-Aldrich 99%), or hydroquinone (1,4-dihydroxybenzene, Sigma-Aldrich 99%) were added to the reactor in 25 cm³ IPA. This was followed by an IPA flush to ensure all reactants entered the reaction mixture, giving a total volume of 350 cm³. The solution was thoroughly mixed and a sample (2.5 cm³) was withdrawn for analysis. The reactor was purged with argon before being purged twice with hydrogen before increasing to the desired reaction pressure (3 barg). The reaction was started by setting the stirrer speed to 1000 rpm and the reaction profile followed by withdrawing samples of 2.5 cm³ over a 180-min time period for each reaction. For the first 30 min a sample was taken every 5 min, this was increased

to every 10 and 20 min for the following 30 and 120 min, respectively. The moles of hydrogen gas consumed during the reaction were also recorded.

Thermo-gravimetric analysis was performed on post-reaction catalysts using a TA Instruments combined TGA/DSC SDT Q600 thermal analyser coupled to an ESS mass spectrometer for evolved gas analysis to investigate catalyst deactivation, specifically carbon deposition on the catalyst. A sample 10–15 mg was heated to a maximum temperature of 1273 K at a ramp rate of 10 deg·min⁻¹ under a 100 cm³·min⁻¹ flow of 2% O₂/Argon. For mass spectrometric analysis, mass fragments: 2 (H₂), 18 (H₂O), 28 (CO), 32 (O₂) and 44 (CO₂) were followed.

4. Conclusions

The hydrogenation and HDO of catechol, resorcinol and hydroquinone over a Rh/silica catalyst has been investigated. Resorcinol was the most active isomer followed by catechol with hydroquinone being the least active. Kinetic analysis revealed that catechol had a negative order of reaction whereas both hydroquinone and resorcinol gave positive half-order suggesting that catechol is more strongly adsorbed. Activation energies of ~30 kJ·mol⁻¹ were determined for catechol and hydroquinone, while resorcinol gave a value of 41 kJ·mol⁻¹. Product analysis revealed that resorcinol and hydroquinone favoured HDO at 323 K and at higher temperatures. In contrast catechol favoured hydrogenation and specifically cis-1,2-dihydroxycyclohexane. This can be explained by the enhanced stability of 1,2-dihydroxycyclohex-1-ene relative to other cyclohexene intermediates of catechol, resorcinol or hydroquinone. This stability facilitates hydrogenation to the cis-isomer relative to tautomerism to the keto form. Trans-isomers are not formed by isomerisation of the equivalent cis-dihydroxycyclohexane but by direct hydrogenation of 2/3/4-hydroxycyclohexanone (Figure 16). The higher selectivity to HDO for resorcinol and hydroquinone may relate to the reactive surface cyclohexenes that have a C=C double bond β-γ to a hydroxyl aiding hydrogenolysis. Using hydrogen instead of deuterium revealed that each isomer had a unique KIE and that HDO to cyclohexane was dramatically affected. The delay in the production of cyclohexane suggest that deuterium acted as an inhibitor and may have blocked the specific HDO site that results in cyclohexane formation [25]. Carbon laydown was detected by post-reaction TPO, revealing three types of surface carbon that were shown to inhibit activity.

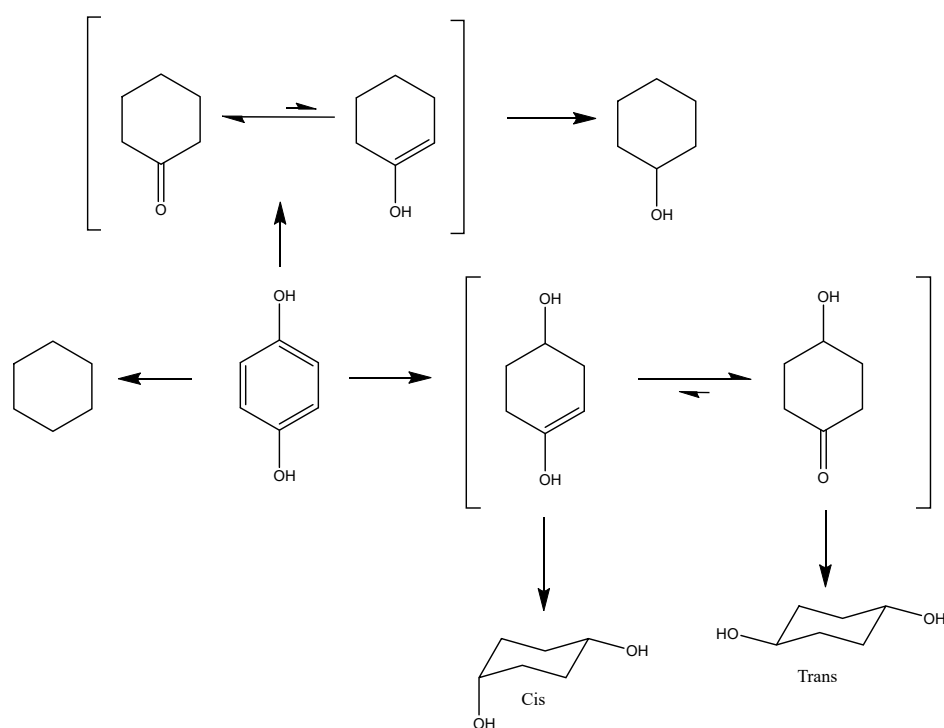


Figure 16. Mechanism for hydrogenation and HDO of hydroquinone.

Supplementary Materials: The following are available online at <http://www.mdpi.com/2073-4344/10/5/584/s1>, Figure S1: Reaction profile of catechol hydrogenation. Conditions, 303 K, 10 mmol, 3 barg. Figure S2: Reaction profile of catechol hydrogenation. Conditions, 343 K, 10 mmol, 3 barg. Figure S3: Activation energy plot for catechol hydrogenation. Figure S4: Reaction profile of resorcinol hydrogenation. Conditions, 333 K, 10 mmol, 3 barg. Figure S5: Activation energy plot for resorcinol hydrogenation. Figure S6: Reaction profile of hydroquinone hydrogenation. Conditions, 303 K, 10 mmol, 3 barg. Figure S7: Reaction profile of hydroquinone hydrogenation. Conditions, 343 K, 10 mmol, 3 barg. Figure S8: Activation energy plot for hydroquinone hydrogenation. Figure S9: Reaction profile of cis-1,2-cyclohexanediol hydrogenation. Conditions, 333 K, 10 mmol, 3 barg. Figure S10: TGA of Rh/SiO₂ catalyst after catechol hydrogenation reaction. Conditions, 10 mmol catechol, 323 K, 3 barg. Figure S11: TGA of Rh/SiO₂ catalyst after resorcinol hydrogenation reaction. Conditions, 10 mmol catechol, 323 K, 3 barg. Figure S12: TGA of Rh/SiO₂ catalyst after hydroquinone hydrogenation reaction. Conditions, 10 mmol catechol, 323 K, 3 barg.

Author Contributions: Conceptualization, S.D.J.; methodology, S.D.J. and K.K.; investigation, K.K.; resources, S.D.J.; writing—original draft preparation, K.K.; writing—review and editing, S.D.J.; supervision, S.D.J. All authors have read and agreed to the published version of the manuscript.

Funding: This work was funded by Innospec Ltd. and University of Glasgow.

Acknowledgments: The authors would like to acknowledge the provision of a studentship for K.K. by Innospec Ltd. and the University of Glasgow.

Conflicts of Interest: The authors declare no conflicts of interest.

References

1. Saidi, M.; Samimi, F.; Karimipourfard, D.; Nimmanwudipong, T.; Gates, B.C.; Rahimpour, M.R. Upgrading of lignin-derived bio-oils by catalytic hydrodeoxygenation. *Energy Environ. Sci.* **2014**, *7*, 103–129. [[CrossRef](#)]
2. Venderbosch, R.; Ardiyanti, A.; Wildschut, J.; Oasmaa, A.; Heeres, H. Stabilization of biomass-derived pyrolysis oils. *J. Chem. Technol. Biotechnol.* **2010**, *85*, 674–686. [[CrossRef](#)]
3. Elkasabi, Y.; Mullen, C.A.; Pighinelli, A.L.; Boateng, A. Hydrodeoxygenation of fast-pyrolysis bio-oils from various feedstocks using carbon-supported catalysts. *Fuel Process. Technol.* **2014**, *123*, 11–18. [[CrossRef](#)]
4. Gunawan, R.; Li, X.; Lievens, C.; Gholizadeh, M.; Chaiwat, W.; Hu, X.; Mourant, D.; Bromly, J.; Li, C.-Z. Upgrading of bio-oil into advanced biofuels and chemicals. Part I. Transformation of GC-detectable light species during the hydrotreatment of bio-oil using Pd/C catalyst. *Fuel* **2013**, *111*, 709–717. [[CrossRef](#)]
5. Kallury, R. Hydrodeoxygenation of hydroxy, methoxy and methyl phenols with molybdenum oxide/nickel oxide/alumina catalyst. *J. Catal.* **1985**, *96*, 535–543. [[CrossRef](#)]
6. Lødeng, R.; Ranga, C.; Rajkhowa, T.; Alexiadis, V.I.; Bjørkan, H.; Chytil, S.; Svenum, I.H.; Walmsley, J.; Thybaut, J.W. Hydrodeoxygenation of phenolics in liquid phase over supported MoO₃ and carburized analogues. *Biomass- Convers. Biorefinery* **2017**, *7*, 343–359. [[CrossRef](#)]
7. Song, W.; Liu, Y.; Barath, E.; Zhao, C.; Lercher, J.A. Synergistic effects of Ni and acid sites for hydrogenation and C–O bond cleavage of substituted phenols. *Green Chem.* **2015**, *17*, 1204–1218. [[CrossRef](#)]
8. Zhao, C.; Kou, Y.; Lemonidou, A.A.; Li, X.; Lercher, J.A. ChemInform Abstract: Hydrodeoxygenation of Bio-Derived Phenols to Hydrocarbons Using RANEY®Ni and Nafion/SiO₂Catalysts. *Chem. Commun.* **2010**, *41*, 412–414. [[CrossRef](#)] [[PubMed](#)]
9. Smith, H.A.; Stump, B.L. A Study of the Catalytic Hydrogenation of Hydroxybenzenes over Platinum and Rhodium Catalysts. *J. Am. Chem. Soc.* **1961**, *83*, 2739–2743. [[CrossRef](#)]
10. Rahaman, M.; Vannice, M.A. The hydrogenation of toluene and o-, m-, and p-xylene over palladium: I. Kinetic behaviour and o-xylene isomerization. *J. Catal.* **1991**, *127*, 251–266.
11. Vasiurrahman, M. The hydrogenation of toluene and o-, m-, and p-xylene over palladium II. Reaction model. *J. Catal.* **1991**, *127*, 267–275. [[CrossRef](#)]
12. AlShehri, F.; Weinert, H.M.; Jackson, S.D. Hydrogenation of alkylaromatics over Rh/silica. *React. Kinet. Mech. Catal.* **2017**, *122*, 699–714. [[CrossRef](#)]
13. Furimsky, E. Catalytic hydrodeoxygenation. *Appl. Catal. A Gen.* **2000**, *199*, 147–190. [[CrossRef](#)]
14. AlShehri, F.; Feral, C.; Kirkwood, K.; Jackson, S.D. Low temperature hydrogenation and hydrodeoxygenation of oxygen-substituted aromatics over Rh/silica: Part 1: Phenol, anisole and 4-methoxyphenol. *React. Kinet. Mech. Catal.* **2019**, *128*, 23–40. [[CrossRef](#)]
15. Smith, H.A.; Thompson, R.G. 73 A Study of the Catalytic Hydrogenation of Methoxybenzenes over Platinum and Rhodium Catalysts. *Adv. Catal.* **1957**, *9*, 727–732. [[CrossRef](#)]

16. Gilman, G.; Cohn, G. The Action of Rhodium and Ruthenium as Catalysts for Liquid-Phase Hydrogenation. *Adv. Catal.* **1957**, *9*, 733–742.
17. Pérez, Y.; Fajardo, M.; Corma, A. Highly selective palladium supported catalyst for hydrogenation of phenol in aqueous phase. *Catal. Commun.* **2011**, *12*, 1071–1074. [[CrossRef](#)]
18. Hurff, S.J.; Klein, M.T. Reaction pathway analysis of thermal and catalytic lignin fragmentation by use of model compounds. *Ind. Eng. Chem. Fundam.* **1983**, *22*, 426–430. [[CrossRef](#)]
19. Toppinen, S.; Rantakylä, T.-K.; Salmi, T.; Aittamaa, J. Kinetics of the Liquid Phase Hydrogenation of Di- and Trisubstituted Alkylbenzenes over a Nickel Catalyst. *Ind. Eng. Chem. Res.* **1996**, *35*, 4424–4433. [[CrossRef](#)]
20. Toppinen, S.; Salmi, T.; Rantakylä, T.-K.; Aittamaa, J. Liquid-Phase Hydrogenation Kinetics of Aromatic Hydrocarbon Mixtures. *Ind. Eng. Chem. Res.* **1997**, *36*, 2101–2109. [[CrossRef](#)]
21. Odebunmi, E. Catalytic hydrodeoxygenation I. Conversions of o-, p-, and m-cresols. *J. Catal.* **1983**, *80*, 56–64. [[CrossRef](#)]
22. Odebunmi, E.; Ollis, D.F. Catalytic hydrodeoxygenation: III. Interactions between catalytic hydrodeoxygenation of m-cresol and hydrodenitrogenation of indole. *J. Catal.* **1983**, *80*, 76–89. [[CrossRef](#)]
23. Bredenberg, J.B.-S.; Sarbak, Z. Infrared studies of the interaction between dihydroxybenzenes and their ethers with the surfaces of γ -Al₂O₃, MoS₂ and a CoMo/ γ -Al₂O₃ catalyst. *J. Chem. Technol. Biotechnol.* **2007**, *42*, 221–234. [[CrossRef](#)]
24. Maximov, A.; Zolotukhina, A.; Murzin, V.; Karakhanov, E.; Rosenberg, E. Ruthenium Nanoparticles Stabilized in Cross-Linked Dendrimer Matrices: Hydrogenation of Phenols in Aqueous Media. *ChemCatChem* **2015**, *7*, 1197–1210. [[CrossRef](#)]
25. Duong, N.N.; Aruho, D.; Wang, B.; Resasco, D.E. Hydrodeoxygenation of anisole over different Rh surfaces. *Chin. J. Catal.* **2019**, *40*, 1721–1730. [[CrossRef](#)]
26. Wey, J.P.; Neely, W.C.; Worley, S.D. Infrared Spectroscopy at High Pressure: Interaction of H₂ and D₂ with Rh/Al₂O₃. *J. Phys. Chem.* **1991**, *95*, 8881–8886. [[CrossRef](#)]
27. Gault, F.G.; Kemball, C. Catalytic exchange of n-hexane and deuterium and some allied reactions on films of palladium and rhodium. *Trans. Faraday Soc.* **1961**, *57*, 1781. [[CrossRef](#)]



© 2020 by the authors. Licensee MDPI, Basel, Switzerland. This article is an open access article distributed under the terms and conditions of the Creative Commons Attribution (CC BY) license (<http://creativecommons.org/licenses/by/4.0/>).